Application of dual-parameter MRI-based radiomics in the differentiation of prostate cancer and benign prostatic hyperplasia: Diagnostic efficacy and predictive modeling

Y. Hu[1,2#], C. Hou[3#], M. Wen[1*]

[1]*Department of Radiology,The First Affiliated Hospital of Chongqing Medical University, Chongqing, China*
[2]*Department of Radiology, The First Hospital of Neijiang, Neijiang, Sichuan, China*
[3]*Department of Oncology, The First Hospital of Neijiang, Neijiang, Sichuan, China*

► ***Original article***

***Corresponding author:**
Ming Wen, M.D.,
***E-mail:** mingwen_dc@163.com*

Received: September 2024
Final revised: February 2025
Accepted: April 2025

Int. J. Radiat. Res., October 2025; 23(4): 907-912

DOI: 10.61186/ijrr.23.4.11

Keywords: *Prostatic neoplasms, radiomics, diffusion magnetic resonance imaging, computer-assisted, machine learning.*

[#]Yanning Hu and Chenliang Hou contributed equally to this work.

ABSTRACT

Background: Prostate cancer (PCa) and benign prostatic hyperplasia (BPH) present with similar clinical symptoms, particularly in patients with borderline prostate-specific antigen (PSA) levels (4–10 ng/mL), making accurate diagnosis challenging. MRI-based radiomics enables non-invasive extraction of quantitative imaging features that may aid in differentiating these conditions. ***Materials and Methods:*** In this retrospective study, 150 patients (56 PCa, 94 BPH) underwent prostate MRI including T2-weighted imaging (T2WI) and diffusion-weighted imaging (DWI). Radiomics features were extracted from manually segmented lesions using PyRadiomics. Logistic regression was used for feature selection and model construction. Three predictive models were developed based on T2WI, DWI, and combined T2WI+DWI features. Model performance was assessed using receiver operating characteristic (ROC) analysis, evaluating area under the curve (AUC), sensitivity, and specificity on training and validation sets. ***Results:*** The combined T2WI+DWI model showed the best diagnostic performance with an AUC of 0.942 in the validation set, sensitivity of 0.821, and specificity of 1.000. This outperformed model based on T2WI or DWI alone, as well as the clinical model using PSA and prostate volume. ***Conclusion:*** Dual-parameter MRI-based radiomics enhances the non-invasive differentiation of PCa from BPH. The combined T2WI and DWI model offers superior diagnostic accuracy and may reduce unnecessary biopsies in patients with indeterminate PSA levels.

INTRODUCTION

Prostate cancer (PCa) is one of the most prevalent malignant tumors affecting men globally, and its early diagnosis and accurate classification are critical for improving patient prognosis [1]. While the disease often presents with similar clinical symptoms to benign prostatic hyperplasia (BPH), the treatment strategies for these conditions differ significantly [2]. Accurate differentiation between PCa and BPH is crucial to prevent over-diagnosis and under-diagnosis, which could lead to inappropriate treatment decisions [3, 4]. Traditional diagnostic methods, such as digital rectal examination (DRE) and prostate-specific antigen (PSA) testing, are widely used for the initial detection of prostate abnormalities [3]. However, these methods have limitations in sensitivity and specificity, which often result in over-treatment of indolent cases and under-treatment of aggressive PCa [5]. For example, elevated PSA levels may be seen in both PCa and BPH, making it challenging to distinguish between the two based solely on PSA levels, especially within the range of 4-10 ng/ml [6]. Therefore, there is a pressing need for more advanced imaging techniques and predictive models to improve diagnostic accuracy and reduce unnecessary biopsies [7].

Magnetic resonance imaging (MRI) has emerged as a valuable tool in prostate cancer diagnosis and management [8]. Among the various MRI sequences, T2-weighted imaging (T2WI) provides excellent anatomical detail and is widely used for detecting prostate lesions, while diffusion-weighted imaging (DWI) offers insights into tissue microstructure by measuring water molecule diffusion [9]. The combination of T2WI and DWI, along with the application of radiomics, allows for the extraction of quantitative imaging features that capture the heterogeneity of prostate lesions [10]. Radiomics, a high-throughput approach, converts medical images into mineable data, enabling the development of models that leverage these imaging features to improve diagnostic precision [11]. The integration of radiomics with advanced machine learning algorithms and multi-parametric MRI (mpMRI) has shown promise in distinguishing PCa from BPH, providing a more nuanced and non-invasive approach to prostate disease management [12].

The primary objective of this study is to evaluate the utility of a dual-parameter MRI-based radiomics model, incorporating features from T2WI and DWI, in differentiating PCa from BPH among patients with

[DOI: 10.61186/ijrr.23.4.11]

PSA levels ranging from 4-10 ng/ml [13]. This study aims to construct predictive models using radiomics features extracted from T2WI and DWI sequences, analyze their diagnostic efficacy, and compare their performance with conventional clinical models based on PSA and other clinical parameters [14]. By leveraging the combined strength of multi-parametric MRI features and radiomics analysis, the study seeks to establish a reliable non-invasive diagnostic tool that can guide clinical decision-making and reduce the need for invasive biopsy procedures [15]. Through this research, we aim to contribute to the growing body of knowledge on the application of advanced imaging techniques in prostate disease diagnosis and demonstrate the potential of radiomics-based models in improving patient outcomes [16].

To our knowledge, this is one of the few studies that systematically evaluates the diagnostic efficacy of a dual-parameter radiomics model combining T2-weighted imaging (T2WI) and diffusion-weighted imaging (DWI) specifically in patients with borderline PSA levels (4–10 ng/mL)—a subgroup where diagnostic uncertainty is especially high. Unlike prior studies that either focused on a single MRI sequence or did not stratify by PSA range, our model integrates high-dimensional radiomics features from both modalities to enhance classification performance. The resulting model demonstrated superior accuracy, sensitivity, and specificity compared to single-sequence and clinical models, offering a novel non-invasive approach that could substantially reduce unnecessary biopsies and improve clinical decision-making in equivocal cases.

MATERIALS AND METHODS

Study design and ethical approval

This was a retrospective observational study approved by the Ethics Committee of Chongqing Medical University (Approval No. Cqmu2022sy; Date of approval: March 28, 2022), conducted in accordance with the Declaration of Helsinki. Written informed consent was obtained from all participants.

Patient selection

A total of 150 male patients who underwent prostate MRI at the First Affiliated Hospital of Chongqing Medical University between January 2021 and December 2022 were included. The inclusion criteria were:

- PSA levels between 4–10 ng/mL,
- Histopathological confirmation of diagnosis via biopsy or surgery,
- Availability of high-quality T2-weighted and diffusion-weighted MRI images.

Patients were excluded if they had a history of prostate surgery, prior prostate cancer treatment (e.g., radiation, hormonal therapy), or incomplete clinical or imaging data.

The study cohort consisted of:

- 56 patients diagnosed with prostate cancer (PCa) based on histopathology, and
- 94 patients with benign prostatic hyperplasia (BPH) confirmed by biopsy or clinical follow-up.

MRI acquisition protocol

All MRI scans were performed using a 3.0 Tesla MRI scanner (MAGNETOM Skyra, Siemens Healthineers, Erlangen, Germany) without the use of contrast agents. The imaging protocol included:

- T2-weighted imaging (T2WI): axial, sagittal, and coronal planes; TR/TE = 4200/102 ms; slice thickness = 3 mm; FOV = 200 mm.
- Diffusion-weighted imaging (DWI): axial plane; b-values = 0 and 1000 s/mm^2; TR/TE = 4800/90 ms; slice thickness = 3 mm.

All images were reviewed and confirmed by two board-certified radiologists with over 5 years of experience in prostate MRI. Regions of interest (ROIs) were manually segmented on T2WI and DWI images using ITK-SNAP software (version 3.8.0; www.itksnap.org, USA).

Radiomics feature extraction

After ROI delineation, radiomics features were extracted using the PyRadiomics package (version 3.0.1; GitHub repository, Netherlands Cancer Institute), implemented in Python (v3.9). Features included first-order statistics, texture features (GLCM, GLRLM, GLSZM, etc.), and wavelet-transformed features. Each MRI modality (T2WI and DWI) was processed independently for feature extraction.

All images were resampled to a voxel size of 1×1×1 mm^3 and normalized prior to feature computation to ensure consistency.

Feature selection and model construction

Initial feature reduction was performed using variance thresholding and correlation filtering. Subsequently, logistic regression analysis with L1 regularization (LASSO) was employed for feature selection and model construction.

Three predictive models were developed:

- T2WI radiomics model,
- DWI radiomics model,
- Combined T2WI + DWI radiomics model.

A fourth clinical model was also developed using PSA, prostate volume, and PSA density (PSAD) for comparison. The dataset was randomly divided into a training set (70%) and a validation set (30%) using stratified sampling to maintain class balance.

Model evaluation

Model performance was evaluated using receiver operating characteristic (ROC) analysis. The

[DOI: 10.61186/ijrr.23.4.11]

following metrics were calculated for both training and validation sets:

- Area under the ROC curve (AUC),
- Sensitivity,
- Specificity.

Calibration curves and nomograms were also constructed using the scikit-learn and statsmodels libraries in Python to assess model fit and clinical applicability.

RESULTS

Clinical and pathological characteristics of patients

The final study population included 150 patients, comprising 56 with histologically confirmed prostate cancer (PCa) and 94 with benign prostatic hyperplasia (BPH). Clinical and pathological parameters are summarized in table 1.

Table 1. Clinical and pathological characteristics of PCa and BPH patients.

Indicator	PCa (n=56)	BPH (n=94)	t-value	P-value
Age (years)	66.74±7.26	65.32±6.93	0.821	0.182
PSA level (ng/ml)	7.41±1.64	7.12±1.35	0.456	0.548
Prostate volume (ml)	48.26±27.13	66.78±29.64	10.248	<0.001
Superior-Inferior Length (cm)	4.12±1.35	4.87±1.42	3.256	0.012
Left-Right Diameter (cm)	3.89±0.96	4.56±0.83	1.983	0.072
Anterior-Posterior Diameter (cm)	5.02±0.72	5.63±0.91	1.725	0.091
PSAD (ng/ml/cm³)	0.21±0.13	0.13±0.08	3.872	0.007

This table compares demographic and clinical features between the prostate cancer and benign prostatic hyperplasia groups. PSA – prostate-specific antigen; PSAD – PSA density; Pca – prostate cancer; BPH – benign prostatic hyperplasia.

There were no statistically significant differences in age or PSA levels between the PCa and BPH groups ($P > 0.05$). However, PCa patients exhibited significantly smaller prostate volumes (mean: 48.26 ± 27.13 mL vs. 66.78 ± 29.64 mL, $P < 0.001$) and higher PSA density (PSAD) values (0.21 ± 0.13 ng/mL/cm^3 vs. 0.13 ± 0.08 ng/mL/cm^3, $P = 0.007$). These differences support the use of prostate volume and PSAD as supplementary clinical indicators.

Radiomics feature selection and model construction

Radiomics features were extracted from manually segmented T2WI and DWI images. After dimensionality reduction using LASSO logistic regression, three features were retained for model construction (table 2):

- T2_wavelet.LHH_glcm_Imc2 (T2WI texture feature),
- DWI_wavelet.LHL_glcm_Idmn (DWI texture feature),
- T2_wavelet.LHH_glcm_MCC (T2WI wavelet-based feature).

These features exhibited measurable differences in patients with PCa versus BPH and were included in the combined radiomics model.

Table 1. Clinical and pathological characteristics of PCa and BPH patients.

Radiomics Feature	Coefficient	Odds Ratio (OR)	95% Confidence Interval (CI)	P-value
T2_wavelet.LHH_glcm_Imc2	1.128	3.115	0.248-51.364	0.387
DWI_wavelet.LHL_glcm_Idmn	-0.278	0.812	0.241-2.357	0.582
T2_wavelet.LHH_glcm_MCC	1.213	3.357	0.813-13.357	0.061

Features were selected through logistic regression from the T2WI and DWI datasets. Abbreviations: OR – odds ratio; CI – confidence interval; T2WI – T2-weighted imaging; DWI – diffusion-weighted imaging; glcm – gray-level co-occurrence matrix; MCC – maximal correlation coefficient; Imc2 – informational measure of correlation 2; Idmn – inverse difference moment normalized.

Diagnostic performance of radiomics and clinical models

Four models were compared: a clinical model (PSA, PSAD, prostate volume), T2WI-only radiomics model, DWI-only radiomics model, and a combined T2WI+DWI radiomics model. Performance metrics are presented in table 3.

Table 3. Diagnostic performance of clinical and radiomics models in training and validation sets.

Model	Training Set AUC	Sensitivity	Specificity	Validation Set AUC	Sensitivity	Specificity
Clinical Model	0.678	0.801	0.631	0.871	0.734	0.526
T2WI Model	0.861	0.873	0.792	0.857	0.871	0.764
DWI Model	0.832	0.741	0.813	0.947	0.874	0.885
Combined T2WI+DWI	0.889	0.875	0.848	0.942	0.821	1.000

The table summarizes AUC, sensitivity, and specificity for all predictive models. AUC – area under the curve; T2WI – T2-weighted imaging; DWI – diffusion-weighted imaging; PCa – prostate cancer; BPH – benign prostatic hyperplasia.

The combined T2WI+DWI model achieved the highest diagnostic performance in the validation set, with an AUC of 0.942, sensitivity of 0.821, and specificity of 1.000.

The DWI-only model also performed well (AUC: 0.947), but with slightly lower specificity.

The clinical model showed the lowest performance (AUC: 0.871; specificity: 0.526).

These findings are illustrated in figure 1, which presents the ROC curves for each model. Figure 2 shows calibration curves, demonstrating that the combined model also had the best calibration (agreement between predicted and observed probabilities).

A nomogram based on the combined T2WI+DWI model is presented in figure 3, enabling individualized risk estimation for PCa. Figure 4 compares model metrics (AUC, sensitivity, specificity) graphically across all models, confirming the superior diagnostic utility of the combined radiomics model.

[DOI: 10.61186/ijrr.23.4.11]

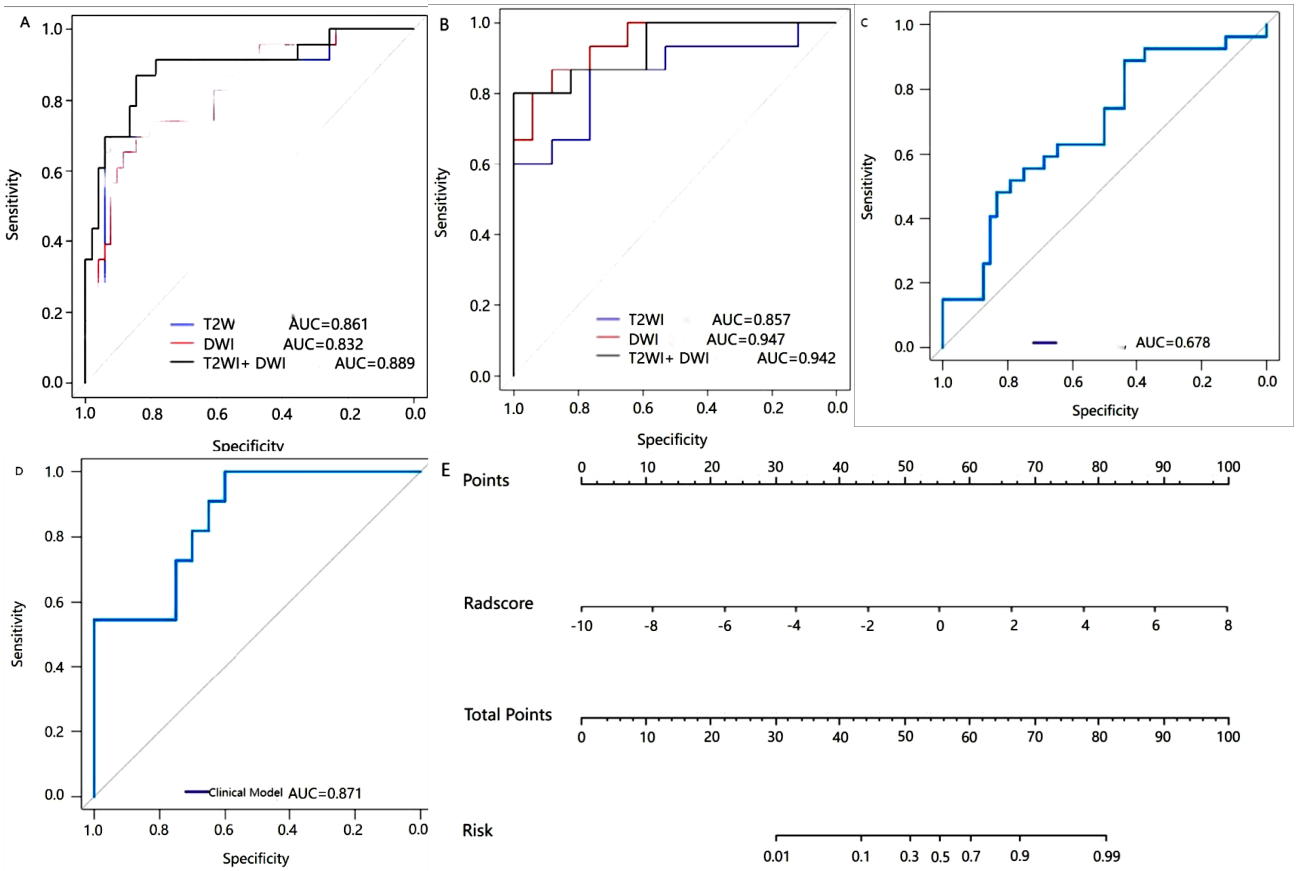

Figure 1. ROC curves for predictive models in the training and validation sets. **(A–B)** ROC curves of the radiomics models (T2WI, DWI, combined) in training and validation cohorts. **(C–D)** ROC curves for the clinical model. **(E)** Nomogram-based prediction model derived from combined T2WI and DWI features. Abbreviations: ROC – receiver operating characteristic; AUC – area under the curve; T2WI – T2-weighted imaging; DWI – diffusion-weighted imaging; PCa – prostate cancer; BPH – benign prostatic hyperplasia.

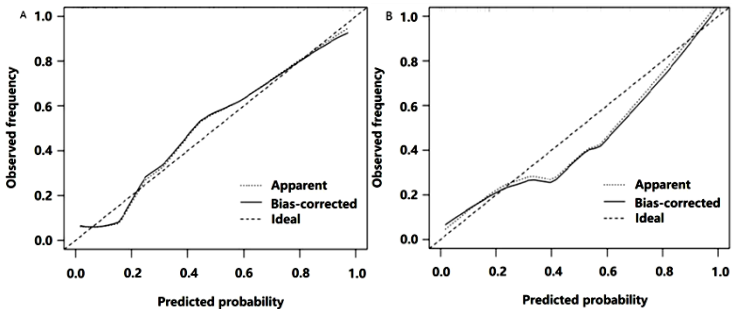

Figure 2. Calibration curves for predictive models. **(A)** Calibration curve for the training set; **(B)** for the validation set. The combined T2WI+DWI model shows the closest alignment between predicted and actual probabilities, indicating high model calibration.

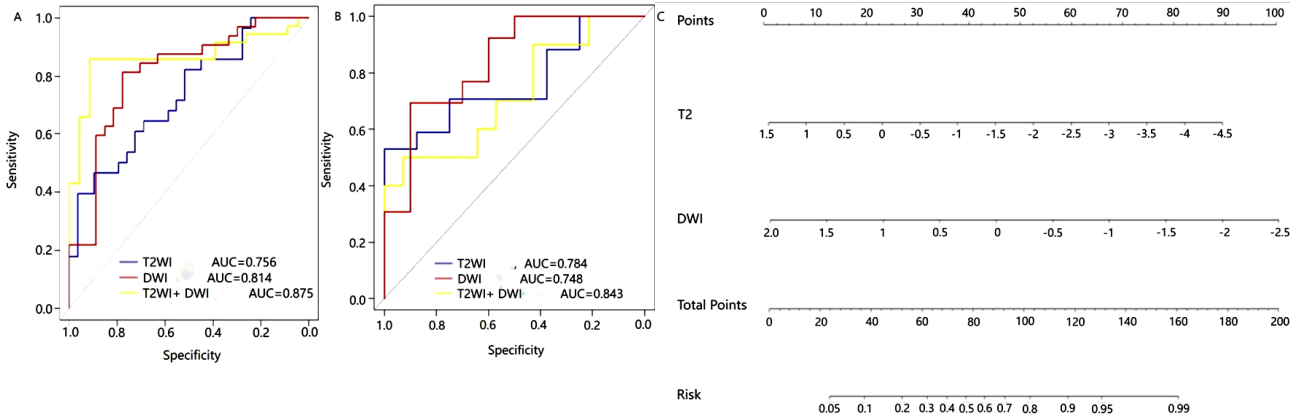

Figure 3. Nomogram based on combined T2WI and DWI radiomics features. The nomogram provides a visual tool to predict the probability of PCa using radiomics scores. Applicable in clinical settings to estimate malignancy risk in patients with PSA values between 4–10 ng/mL.

[DOI: 10.61186/ijrr.23.4.11]

DISCUSSION

The results of this study indicate that the radiomics models based on T2-weighted imaging (T2WI) and diffusion-weighted imaging (DWI) are highly effective in distinguishing prostate cancer (PCa) from benign prostatic hyperplasia (BPH) [17]. The combined T2WI and DWI model demonstrated superior diagnostic performance compared to single-modality models in terms of area under the curve (AUC), sensitivity, and specificity [18]. The AUC of the combined model was 0.942 in the validation set, significantly higher than the AUCs of the T2WI-only and DWI-only models [19]. This suggests that combining features from both modalities captures more comprehensive information about the prostate tissue, leading to improved classification accuracy. The T2WI modality provides anatomical and structural information, while DWI captures changes in tissue microstructure, which are often indicative of malignancy. The complementary nature of these modalities enhances the model's ability to differentiate between PCa and BPH, reducing false-positive and false-negative rates and providing a more reliable diagnostic tool for clinical use [20].

The sensitivity and specificity of the combined model were 0.821 and 1.000, respectively, in the validation set, indicating that the model is highly sensitive to detecting PCa while maintaining perfect specificity [21]. This performance suggests that the radiomics features extracted from T2WI and DWI can identify subtle differences between PCa and BPH that are not visible to the naked eye, even for experienced radiologists. The integration of these imaging features into a predictive model could potentially reduce the number of unnecessary biopsies for patients with elevated PSA levels, particularly those with borderline PSA values between 4-10 ng/ml [22]. The findings of this study support the hypothesis that combining multi-parametric MRI features can enhance the diagnostic performance of radiomics models, paving the way for more personalized and precise prostate disease management [17].

The potential application of radiomics features in grading prostate cancer was also explored in this study [23]. The combined T2WI and DWI model demonstrated excellent performance in distinguishing low-grade PCa (Gleason score ≤6) from high-grade PCa (Gleason score ≥7), with an AUC of 0.934 in the validation cohort. This finding indicates that radiomics features can serve as non-invasive imaging biomarkers for assessing tumor aggressiveness and guiding treatment decisions [24]. Radiomics features such as T2_wavelet. LHH_glcm_Imc2 and DWI_wavelet.LHL_glcm_Idmn, which were selected in the combined model, were found to be significantly associated with higher Gleason scores, reflecting their potential to capture the microstructural and textural complexity of aggressive tumors [25]. The ability to accurately grade PCa using non-invasive imaging techniques is critical, as it helps clinicians stratify patients into appropriate risk categories, identify candidates for active surveillance, and select those who may benefit from more aggressive treatment modalities [26].

The results also showed a strong correlation between specific radiomics features and Gleason scores, suggesting that these imaging biomarkers could potentially complement traditional histopathological evaluations. The use of radiomics features to grade PCa non-invasively could reduce the reliance on biopsy procedures, which carry the risk of complications and sampling errors [27]. Moreover, radiomics-based grading can be performed repeatedly over time to monitor disease progression or response to therapy, making it a valuable tool for long-term patient management [28].

This study is limited by its single-center, retrospective design and relatively small sample size. Manual ROI delineation may introduce inter-observer variability. The cohort included only patients with PSA levels of 4–10 ng/mL, which may restrict generalizability. External validation and the use of automated segmentation tools are needed in future research. Furthermore, although the radiomics features extracted in this study showed significant associations with PCa and BPH, the biological interpretation of these features remains challenging. Future research should focus on elucidating the underlying biological mechanisms represented by these radiomics features, which would enhance their clinical utility and facilitate their integration into routine diagnostic workflows. Additionally, incorporating other advanced imaging modalities such as contrast-enhanced MRI or MR spectroscopy could provide additional information to further improve the diagnostic and prognostic value of radiomics models.

CONCLUSION

Dual-parameter MRI-based radiomics, combining T2WI and DWI features, significantly enhances the diagnostic accuracy for differentiating PCa from BPH. The model offers a reliable, non-invasive tool with potential to reduce unnecessary biopsies in patients with borderline PSA levels. Further validation in multi-center settings is warranted to confirm clinical utility.

***Acknowledgments*:** The authors extend their sincere thanks to the radiologists, pathologists, and research staff at the First Affiliated Hospital of Chongqing Medical University for their invaluable assistance with data acquisition, imaging review, and technical support.

***Conflict of Interest*:** The authors declare that they

[DOI: 10.61186/ijrr.23.4.11]

have no conflicts of interest relevant to this study.

***Funding*:** This study did not receive any funding from public, commercial, or non-profit agencies.

***Ethical Considerations*:** This study was approved by the Ethics Committee of Chongqing Medical University (Approval No. Cqmu2022sy, issued on March 28, 2022), and was conducted in accordance with the Declaration of Helsinki. All participants provided written informed consent prior to inclusion in the study.

***Clinical Registration*:** Not applicable.

***Availability of Data and Materials*:** The datasets generated and analyzed during the current study are available from the corresponding author upon reasonable request.

***Authors' Contributions*:** M.W.: Conceptualization, project supervision, final approval. Y.H. and C.H.: Data collection, image segmentation, statistical analysis, model development, and manuscript drafting. All authors have read and approved the final manuscript and agree to be accountable for all aspects of the work.

***Consent for Publication*:** All authors have provided consent for publication.

***AI Use Statement*:** Artificial intelligence tools were used exclusively for improving language clarity, formatting, and editing of the manuscript. No AI tool was used for data analysis, interpretation, or generation of scientific content.

REFERENCES

1. Berenguer CV, Pereira F, Câmara JS, Pereira JAM (2023) Underlying features of prostate cancer-statistics, risk factors, and emerging methods for its diagnosis. *Curr Oncol,* ***30****(2): 2300-21*.
2. Miernik A and Gratzke C (2020) Current treatment for benign prostatic hyperplasia. *Dtsch Arztebl Int,* ***117****(49): 843-54.*
3. Mottet N, Bellmunt J, Bolla M, Briers E, Cumberbatch MG, De Santis M, *et al.* (2017) EAU-ESTRO-SIOG Guidelines on prostate cancer. Part 1: Screening, diagnosis, and local treatment with curative intent. *Eur Urol,* ***71****(4): 618-29*.
4. Siegel RL, Miller KD, Fuchs HE, Jemal A (2021) Cancer Statistics, 2021. *CA Cancer J Clin,* ***71****(1): 7-33*.
5. Schröder FH, Hugosson J, Roobol MJ, Tammela TL, Ciatto S, Nelen V, *et al.* (2009) Screening and prostate-cancer mortality in a randomized European study. *N Engl J Med,* ***360****(13): 1320-8*.
6. Loeb S, Bjurlin MA, Nicholson J, Tammela TL, Penson DF, Carter HB, *et al.* (2014) Overdiagnosis and overtreatment of prostate cancer. *Eur Urol,* ***65****(6): 1046-55*.
7. Barry MJ and Simmons LH (2017) Prevention of prostate cancer morbidity and mortality: Primary prevention and early detection. *Med Clin North Am,* ***101****(4): 787-806*.
8. Fernandes MC, Yildirim O, Woo S, Vargas HA, Hricak H (2022) The role of MRI in prostate cancer: current and future directions. *Magma,* ***35****(4): 503-21*.
9. Barentsz JO, Weinreb JC, Verma S, Thoeny HC, Tempany CM, Shtern F, *et al.* (2016) Synopsis of the PI-RADS v2 Guidelines for multiparametric prostate magnetic resonance imaging and recommendations for use. *Eur Urol,* ***69****(1): 41-9*.
10. Ahmed HU, El-Shater Bosaily A, Brown LC, Gabe R, Kaplan R, Parmar MK, *et al.* (2017) Diagnostic accuracy of multi-parametric MRI and TRUS biopsy in prostate cancer (PROMIS): a paired validating confirmatory study. *Lancet,* ***389****(10071): 815-22*.
11. Gillies RJ, Kinahan PE, Hricak H (2016) Radiomics: Images are more than pictures, they are data. R*adiology,* ***278****(2): 563-77*.
12. Li C, Deng M, Zhong X, Ren J, Chen X, Chen J, *et al.* (2023) Multi-view radiomics and deep learning modeling for prostate cancer detection based on multi-parametric MRI. *Front Oncol,* ***13****: 1198899.*
13. Cuocolo R, Cipullo MB, Stanzione A, Ugga L, Romeo V, Radice L, *et al.* (2019) Machine learning applications in prostate cancer magnetic resonance imaging. *Eur Radiol Exp,* ***3****(1): 35*.
14. van der Leest M, Cornel E, Israël B, Hendriks R, Padhani AR, Hoogenboom M, *et al.* (2019) Head-to-head comparison of transrectal ultrasound-guided prostate biopsy versus multiparametric prostate resonance imaging with subsequent magnetic resonance-guided biopsy in biopsy-naïve men with elevated prostate-specific antigen: A large prospective multicenter clinical study. *Eur Urol,* ***75****(4): 570-8.*
15. Lee HW, Kim E, Na I, Kim CK, Seo SI, Park H (2023) Novel multiparametric magnetic resonance imaging-based deep learning and clinical parameter integration for the prediction of long-term biochemical recurrence-free survival in prostate cancer after radical prostatectomy. C*ancers (Basel),* ***15****(13): 3416*
16. Felker ER, Margolis DJ, Nassiri N, Marks LS (2016) Prostate cancer risk stratification with magnetic resonance imaging. *Urol Oncol,* ***34*** *(7): 311-9*.
17. Algohary A, Viswanath S, Shiradkar R, Ghose S, Pahwa S, Moses D, *et al.* (2018) Radiomic features on MRI enable risk categorization of prostate cancer patients on active surveillance: Preliminary findings. *J Magn Reson Imaging,* ***48****(3): 818-828.*
18. Lambin P, Rios-Velazquez E, Leijenaar R, Carvalho S, van Stiphout RG, Granton P, *et al.* (2012) Radiomics: extracting more information from medical images using advanced feature analysis. *Eur J Cancer,* ***48****(4): 441-6.*
19. Fütterer JJ, Briganti A, De Visschere P, Emberton M, Giannarini G, Kirkham A, *et al.* (2015) Can clinically significant prostate cancer be detected with multiparametric magnetic resonance imaging? A systematic review of the literature. *Eur Urol,* ***68****(6): 1045-53*.
20. Haider MA, Brown J, Yao X, Chin J, Perlis N, Schieda N, *et al.* (2021) Multiparametric Magnetic resonance imaging in the diagnosis of clinically significant prostate cancer: an updated systematic review. *Clin Oncol (R Coll Radiol),* ***33****(12): e599-e612*.
21. Sun Y, Reynolds HM, Parameswaran B, Wraith D, Finnegan ME, Williams S, *et al.* (2019) Multiparametric MRI and radiomics in prostate cancer: a review. *Australas Phys Eng Sci Med,* ***42****(1): 3-25.*
22. Yoo S, Kim JK, Jeong IG (2015) Multiparametric magnetic resonance imaging for prostate cancer: A review and update for urologists. *Korean J Urol,* ***56****(7): 487-97*.
23. Chaddad A, Kucharczyk MJ, Cheddad A, Clarke SE, Hassan L, Ding S, *et al.* (2021) Magnetic resonance imaging based radiomic models of prostate cancer: A narrative review. *Cancers (Basel),* ***13****(3): 552.*
24. Ferro M, de Cobelli O, Vartolomei MD, Lucarelli G, Crocetto F, Barone B, *et al.* (2021) Prostate cancer radiogenomics-from imaging to molecular characterization. *Int J Mol Sci,* ***22****(18): 9971.*
25. He X, Xiong H, Zhang H, Liu X, Zhou J, Guo D (2021) Value of MRI texture analysis for predicting new Gleason grade group. *Br J Radiol,* ***94****(1121): 20210005*.
26. Stanzione A, Gambardella M, Cuocolo R, Ponsiglione A, Romeo V, Imbriaco M (2020) Prostate MRI radiomics: A systematic review and radiomic quality score assessment. *European Journal of Radiology,* ***129****: 109095*.
27. Bonekamp D, Kohl S, Wiesenfarth M, Schelb P, Radtke JP, Götz M, *et al.* (2018) Radiomic machine learning for characterization of prostate lesions with mri: comparison to ADC values. *Radiology,* ***289****(1): 128-37.*
28. Fan X, Xie N, Chen J, Li T, Cao R, Yu H, *et al.* (2022) Multiparametric MRI and machine learning based radiomic models for preoperative prediction of multiple biological characteristics in prostate cancer. *Front Oncol,* ***12****: 839621*.

[DOI: 10.61186/ijrr.23.4.11]